Aging Cell (2011) **10,** pp1056–1066 Doi: 10.1111/j.1474-9726.2011.00749.x

Alteration in *N*-glycomics during mouse aging: a role for FUT8

Valerie Vanhooren,[1,2] Sylviane Dewaele,[1,2] Makoto Kuro-o,[3] Naoyuki Taniguchi,[4] Laurent Dollé,[5] Leo A. van Grunsven,[5] Evgenia Makrantonaki,[6,7] Christos C. Zouboulis,[6] Cuiying C. Chen[1,2] and Claude Libert[1,2]

[1]Department for Molecular Biomedical Research, VIB, Technologiepark 927, 9000, Ghent, Belgium
[2]Department of Biomedical Molecular Biology, Ghent University, Technologiepark 927, 9000, Ghent, Belgium
[3]Department of Pathology, The University of Texas Southwestern Medical Center at Dallas, 5323 Harry Hines Blvd., Dallas, TX 75390-9072, USA
[4]Systems Glycobiology Research Group, Department of Chemical Biology, RIKEN Advanced Science Institute, 2-1 Hirosawa, Wako, Saitama, Japan
[5]Liver Cell Biology Lab, Department of Cell Biology, Vrije Universiteit Brussel (VUB), Laarbeeklaan 103, 1090, Brussels, Belgium
[6]Departments of Dermatology, Venereology, Allergology and Immunology, Dessau Medical Center, 38 Auenweg, 06847, Dessau, Germany
[7]Laboratory for Biogerontology, Dermato-Pharmacology and Dermato-Endocrinology, Institute of Clinical Pharmacology and Toxicology, Charité Universitaetsmedizin Berlin, Campus Benjamin Franklin, 30 Hindenburgdamm, 12200, Berlin, Germany

Summary

We recently reported that *N*-glycosylation changes during human aging. To further investigate the molecular basis determining these alterations, the aging process in mice was studied. *N*-glycan profiling of mouse serum glycoproteins in different age groups of healthy C57BL/6 mice showed substantial age-related changes in three major *N*-glycan structures: under-galactosylated biantennary (NGA2F), biantennary (NA2), and core α-1,6-fucosylated -β-galactosylated biantennary structures (NA2F). Mice defective in klotho gene expression (kl/kl), which have a shortened lifespan, displayed a similar but accelerated trend. Interestingly, the opposite trend was observed in slow-aging Snell Dwarf mice (dw/dw) and in mice fed a calorically restricted diet. We also discovered that increased expression and activity of α-1,6-fucosyltransferase (FUT8) in the liver are strongly linked to the age-related changes in glycosylation and that this increased FUT8 and fucosylation influence IGF-1 signaling. These data demonstrate that the glycosylation machinery in liver cells is significantly affected during aging and that age-related increased FUT8 activity could influence the aging process by altering the sensitivity of the IGF-1R signaling pathway.

Key words: *N*-glycan; glycosylation; aging; Snell Dwarf; klotho mouse; caloric restriction.

Introduction

Aging can be defined as progressive functional decline and increasing mortality over time (Lombard *et al.*, 2005). The aging process is partially under genetic control and is influenced by the environment (Mariani *et al.*, 2005; Lautenschlager & Almeida, 2006). Several cellular pathways have been found to be connected to the aging process. These pathways, which either suppress or enhance the aging process, include regulation of the insulin/growth hormone (GH) axis, ROS metabolism, and DNA repair (Andressoo & Hoeijmakers, 2005).

N-linked oligosaccharides of glycoproteins play important biological roles by influencing the functions of glycoproteins (Kukuruzinska & Lennon, 1998). They are important for initiation of various cellular recognition signals that are essential for maintaining the ordered social life of the cells of a multicellular organism, e.g., receptor activation, endocytosis, and cell adhesion (Raman *et al.*, 2005). Although many studies reported the importance of the changes in glycan structures during development and disease (Freeze & Aebi, 2005), little information is available on these changes during aging (Parekh *et al.*, 1988). Because the biosynthesis of glycans is not controlled by interaction with a template but depends on the concerted action of glycosyltransferases and glycosidases, the structure of glycans is much more variable compared with that of proteins and nucleic acids, and they can easily be altered by changes in the physiological condition of the cells.

In our previous studies, we demonstrated that three major *N*-glycan structures (NGA2F, NGA2FB, and NA2F) present in human blood glycoproteins undergo changes during aging (Vanhooren *et al.*, 2007, 2010). These results indicate that the measurement of *N*-glycan levels could provide a noninvasive surrogate marker for general health, for forecasting disease progression upon aging, and for monitoring the efficacy of anti-aging medications.

In this study, we compared the changes in the serum *N*-glycome during aging in genetically identical inbred C57BL/6 mice housed in a specific pathogen-free environment (SPF) to reduce the influence of genetic polymorphisms and the environment to a minimum. To confirm our findings, the serum *N*-glycome of long-lived and short-lived mouse models was compared, and to understand the mechanism driving N-glycosylation alterations, the gene expression levels and protein activity of important glyco-genes were measured.

Results

Serum glycomic profiling of aging healthy C57BL/6 mice

In our previous study, we demonstrated the alteration in serum *N*-glycans during human aging (Vanhooren *et al.*, 2007, 2010). To investigate whether this holds true in mice, we studied the serum *N*-glycome during mouse aging in inbred mice. To do so, eight C57BL/6 male mice per age group (3, 8, 15, and 23 months old) were housed under SPF conditions and bled monthly during 4 months (except that the oldest group was bled monthly during 3 months). Total serum desialylated *N*-glycans were released from glycoproteins after treatment with peptide N-glycosidase F (PNGase F) and then digested with sialidase (see M&M). The desialylated *N*-glycan profiles of different age groups were analyzed by DNA sequencer-assisted, fluorophore-assisted carbohydrate electrophoresis (DSA-FACE). As shown in Fig. 1A, the desialylated *N*-glycan profile contained nine major peaks in C57BL/6 mice. The area under the peaks, that represents the relative concentrations of the oligosaccharide structures, was quantified and normalized to the total signal intensity. By analyzing *N*-glycans of different age groups, we found that three glycan structures are closely linked to aging. Peaks 1 and 6 (Fig. 1B,C) were increased during

Correspondence
Dr Claude Libert and Dr Cuiying Chitty Chen, Department for Biochemical Molecular Biology, Ghent University, VIB, Technologiepark 927, B-9052 Ghent, Belgium. Tel.: +32 93313700; fax: +32 93313609; e-mails: Claude@dmbr.vib-ugent.be; chitty@dmbr.ugent.be

Accepted for publication *9 September 2011*

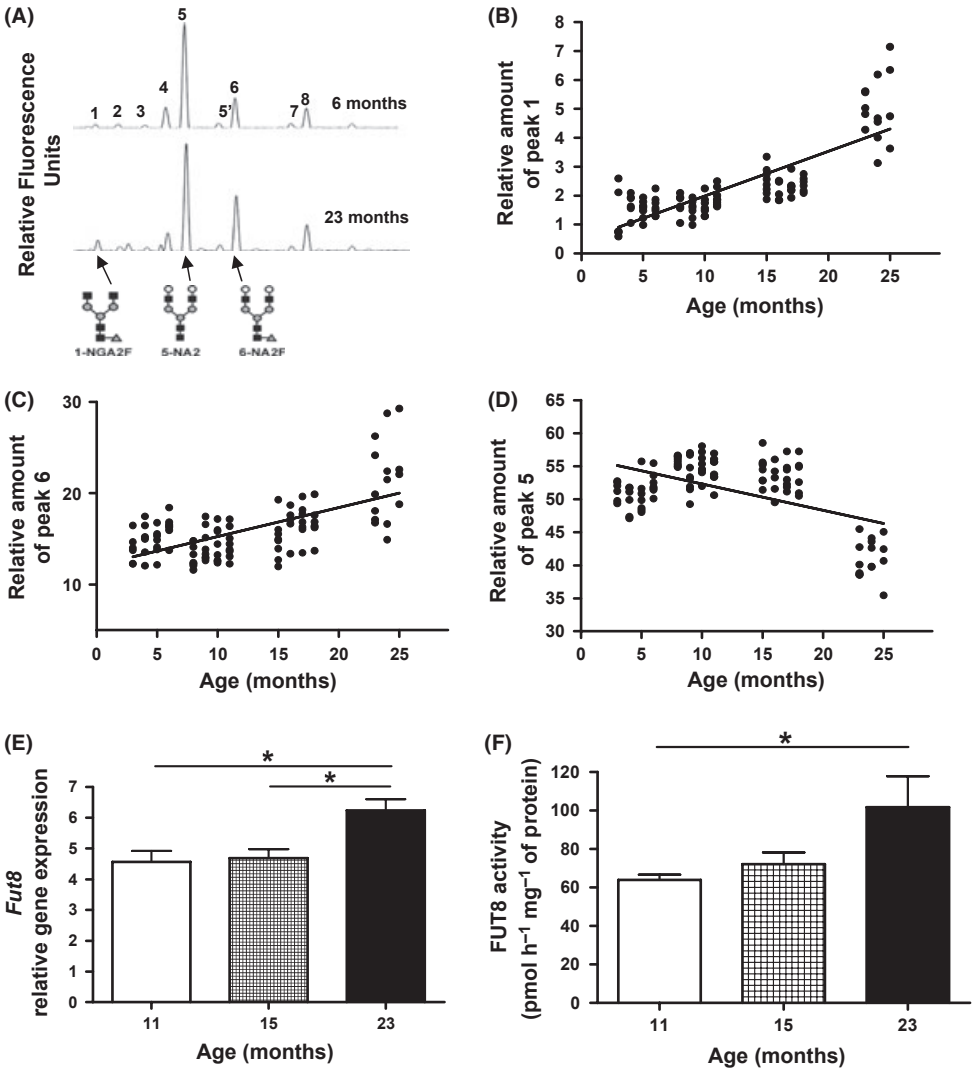

Fig. 1 N-glycosylation alterations in serum proteins and FUT8 expression/activity in the liver of C57BL/6 mice during healthy aging. (A) A typical desialylated *N*-glycan profile is shown for total serum proteins of healthy C57BL/6 mice of 6 months (top panel) and of 23 month (lower panel) old housed in an SPF animal house. The structures of the three most relevant peaks are shown below the panels. Peak 1 is an agalactosylated, core-α-1,6-fucosylated biantennary glycan (NGA2F), peak 5 is a bigalactosylated, biantennary glycan (NA2) and peak 6 is a bigalactosylated, core-α-1,6-fucosylated biantennary glycan (NA2F). *N*-Acetylglucosamine ■, fucose △, mannose ◍, and galactose ○. (B–D) The relative concentrations of the oligosaccharide structures (in percentage), statistically analyzed for correlation between glycans and aging, of C57BL/6 mice during healthy aging. Blood was taken and analyzed with DSA-FACE every month, for 4 months of four age groups (3, 8, 15, and 23 months old) of 8 male C57BL/6 mice. For the oldest age group (start age 23 months), blood was taken only for 3 months as many mice became sick or died. (B) Relative amount of peak 1 in correlation with the age, there is an age-dependent increase of peak 1 ($r = 0.8048$, $P < 0.0001$) (C) relative amount of peak 6 in correlation with the age, there is an age-dependent increase of peak 6 ($r = 0.6276$, $P < 0.0001$), and (D) relative amount of peak 5 in correlation with the age, there is an age-dependent decrease of peak 6 ($r = -0.5232$, $P < 0.0001$). (E–F) The relative gene expression and activity of FUT8 in the liver of healthy aging C57BL/6 mice. (E) *Fut8* gene expression in liver during aging of healthy C57BL/6 mice measured by Q-PCR ($n = 8$ for 11 and 15 months; $n = 7$ for 23 months). A clear age-related upregulation of *Fut8* gene expression was observed. (F) FUT8 activity in the liver during aging of healthy C57BL/6 mice was measured ($n = 4$ in each age group). A clear age-related upregulation of FUT8 activity was observed in correlation with the gene expression.

aging while peak 5 was decreased (Fig. 1D). Most serum *N*-glycoproteins are secreted by the B cells (antibodies) and the liver. To investigate the contribution of antibodies to the changes in peaks 1, 5, and 6, we performed DSA-FACE on antibody-depleted serum from the same aging SPF male C57BL/6 mice. We still found the same age-related N-glycosylation alterations in the antibody-depleted fraction (data not shown), demonstrating that mainly N-glycosylation of proteins secreted by the liver is influenced by age. We performed structural analysis of *N*-glycans using exoglycosidases. In agreement with our previous report (Liu *et al.*, 2010), peak 1 and peak 6 represent agalacto core-α-1,6-fucosylated biantennary (NGA2F) and bigalacto core-α-1,6-fucosylated biantennary (NA2F), respectively, while peak 5 represents bigalacto biantennary structures (NA2).

Increase in fucosylation during aging

As peak 1 and peak 6 contain core-α-1,6-fucose structure and both are increased during aging, we examined total core-α-1,6-fucosylated glycoprotein in serum of C57BL/6 male mice housed in SPF conditions at different ages (11, 15, and 23 months). Western lectin blots of total serum proteins were performed using *Aspergillus oryzae* lectin (AOL) as probe,

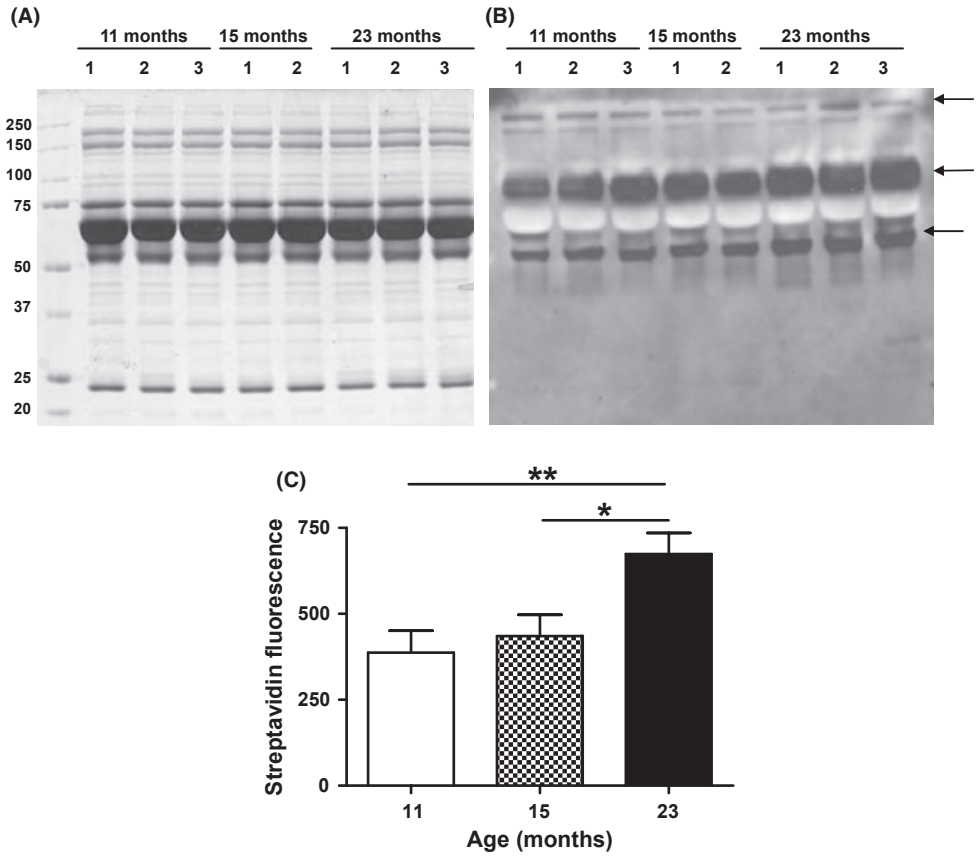

Fig. 2 *Aspergillus oryzae* lectin (AOL) lectin blot of serum from aging C57BL/6 mice. Serum from the healthy male C57BL/6 aging mice of different ages (11, 15, and 23 months old) was subjected to SDS-PAGE. The gel was stained for total protein with coomassie (A) and also blotted to a membrane and probed with an AOL lectin that recognizes α-1,6-core-fucosylated proteins (B). The left lane is the protein marker, and the molecular weight in kDa is indicated. The intensity of numerous AOL bands was increased (marked with an arrow) whereas the amount of protein seen on the coomassie gel remained constant. The intensity of the total AOL bands was measured and plotted out (C). There is a clear increase in α-1,6-core fucosylation on different serum proteins during aging.

which is a carbohydrate-binding protein that recognizes specifically α-1,6-fucosylated glycans (Matsumura *et al.*, 2007). When comparing the AOL staining (Fig. 2B) with a staining for total protein amount (Coomassie Fig. 2A), it becomes clear that not all, but a large amount of proteins in the serum are α-1,6-fucosylated and that a clear age-related increase in AOL bands is detected. As shown in Fig. 2C, where the total AOL band intensity was measured, AOL-binding of serum glycoproteins was gradually increased during aging.

Increased Fut8 gene expression and activity in the liver of aging mice

The liver is the major producer of serum *N*-glycoproteins. To determine whether the increase in serum core-fucosylated glycoproteins was because of altered biosynthesis of the structures in the liver, Q-PCR for glycosylation biosynthesis enzymes in the liver was performed. We focused on alpha-1,6-fucosyltransferase 8 (FUT8) as it has been reported that FUT8, which adds a fucose to core *N*-acetylglucosamine (GlcNAc), is the only fucosyltransferase involved in core fucosylation in mice (Wang *et al.*, 2006b). We investigated whether the increased level of fucosylated glycoprotein in serum of old mice was caused by upregulation of *Fut8* gene expression in liver. Total RNA was prepared of the livers of C57BL/6 mice at the age of 11 months (n = 8), 15 months (n = 8), and 23 months (n = 7). The gene expression was measured using Q-PCR. Indeed, we found that *Fut8* expression was upregulated significantly in the livers of old mice (23 months) compared to younger mice (11 and 15 months; Fig. 1E). The gene expression level of other fucose metabolism genes was also measured, namely those genes coding for fucose transporter, GDP-mannose-4,6-dehydratase, GDP-keto-6-deoxymannose-3,5-epimerase-4-reductase, and GDP-L-fucose synthetase, but no differences were observed during aging (data not shown). The transcriptional regulation of *Fut8* in the liver of old mice was correlated with increased FUT8 biological enzyme activity in old mice (23 months; Fig. 1F). Thus, the increased core fucosylation of glycoprotein in serum is indeed associated with transcriptional increase of *Fut8* in the livers of old mice. This explains at least partly that the increase of peak 1 (NGA2F) and peak 6 (NA2F) during aging is caused by an increased *Fut8* expression in the liver. These results might also explain the decrease in peak 5 (NA2) during aging, because NA2 is used as a substrate by FUT8 to form peak 6 (NA2F).

Caloric restriction prevents the age-related *N*-glycan changes

In mammals, caloric restriction (CR) is an effective way to delay age-related diseases and extend good health into old age. Mice that consume 30–40% fewer calories survive 20–50% longer than mice fed *ad libitum* (AL) (Weindruch *et al.*, 1988). We investigated whether CR can delay or reverse the age-related *N*-glycan changes observed in healthy, aging mice. C57BL/6 mice (n = 8) at the age of 2 months were fed a diet containing 40% less calories than the control group (n = 8) fed *ad libitum* for 6 months. During the first 2 months, the CR mice lost 25% of their bodyweight, after which their bodyweight stabilized (data not shown). Blood was collected monthly. The serum *N*-glycan profiles were generated by DSA-FACE. A clear antiaging inversion of the glycan profile is seen in CR mice in comparison with AL control mice. As peak 1 increases and peak 6 stays stable during the time of measuring in control mice (Fig. 3A,B black), they decreased in CR mice (Fig. 3A,B red). On the other hand, the level of peak 5 increased with age in CR mice compared with control mice

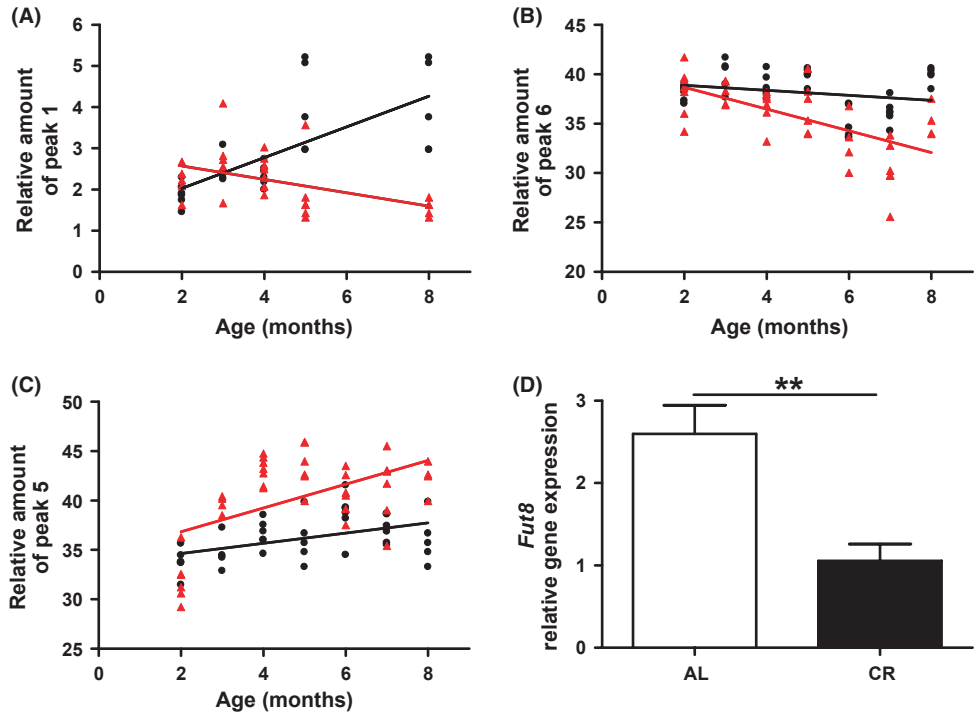

Fig. 3 *N*-glycosylation alterations in serum proteins and FUT8 expression in the liver of AL and CR C57BL/6 mice. The area under the peaks that represents the relative concentrations of the oligosaccharide structures (in percentage) was analyzed statistically for the correlation between glycans, age, and feeding conditions. Blood was taken at 2 months of age, before starting the CR feeding. Afterward, blood was taken every month from the AL (n = 8) and CR groups (n = 8), until 8 months of age. The AL group is presented by the black line and dots and the CR group by the red line and triangles. (A) There is an age-dependent increase of peak 1 in the AL group (r = 0.7024, P < 0.0001), but there is an age-dependent decrease in peak 1 in the CR group (r = −0.4772, P = 0.0089). The difference between the slope of the AL and CR condition is extremely significant, P < 0.0001. (B) There is no change in peak 6 with age in AL conditions over the time frame analyzed here (r = −0.2313, NS) but here is an age-dependent decrease in peak 6 in the CR group (r = −0.6334, P < 0.0001). The difference between the slope of the AL and CR condition is significant, P = 0.003247. (C) There is no change in peak 5 with age in AL conditions over the time frame analyzed here. There is an age-dependent increase in peak 5 in the CR group (r = 0.5382, P = 0.0004). The difference between the slopes of the AL and CR condition is not quite significant, P = 0.05293. (D) The relative gene expression of FUT8 in the liver measured by Q-PCR. Decreased expression of FUT8 in calorie-restricted (CR, n = 7) C57BL/6 mice compared with *ad libitum*-fed (AL, n = 7) C57BL/6 mice.

(Fig. 3C). Moreover, we also observed that CR intervention influences the *Fut8* gene expression in the liver: we found that *Fut8* expression in liver is significantly decreased by CR intervention compared to AL mice (Fig. 3D). Thus, we demonstrate that aging-related changes in *N*-glycans in healthy aging C57BL/6 mice can be prevented by CR.

Evaluation of serum *N*-glycan changes in Snell Dwarf mice and in mice defective in klotho gene expression

To see whether serum *N*-glycan changes during C57BL/6 aging is a general aging biomarker, we investigated the *N*-glycome in two other aging mouse models: Snell Dwarf mice (dw/dw) and mice carrying severe hypomorphic klotho alleles (kl/kl).

Snell Dwarf mice are homozygous for the $Pit1^{dw}$ allele, which eliminates the function of the transcription factor Pit1 (Li *et al.*, 1990). Snell Dwarf mice are deficient in GH, prolactin (PRL), and thyroid-stimulating hormone (TSH) owing to hypoplasia of the cells that produce these hormones in the anterior pituitary. These mice are resistant to chemically induced cancers and live longer than control mice that are either homozygous or heterozygous for the wild-type Pit1 allele (Bielschowsky & Bielschowsky, 1959; Rennels *et al.*, 1965; Flurkey *et al.*, 2001, 2002). In this study, we collected serum longitudinally from homozygous Snell Dwarf mice (dw/dw, n = 10) and control mice (WT, n = 10) during different age time points. As shown in Fig. 4B,C, Dwarf mice have a lower peak 6 and a higher peak 5 compared to age- and sex-matched control mice of the same genetic background. Both the WT and the Dwarf mice demonstrate the age-related trend in peaks 6 and 5 but the amount of peak 6 is always lower and amount of peak 5 is always higher in Dwarf mice compared with age-matched WT mice. In contrast, no difference in peak 1 was observed between Dwarf and control mice (Fig. 4A).

The *klotho* gene is involved in the suppression of several aging phenotypes. A defect in *klotho* gene expression in the mouse generates a syndrome that resembles human premature aging, including a short lifespan, infertility, arteriosclerosis, skin atrophy, osteoporosis, and pulmonary emphysema (Kuro-o *et al.*, 1997). Thus, mice defective in *klotho* gene expression (kl/kl) have been used as a model for human aging. Peak dynamics were also measured in this short-lived mouse to evaluate *N*-glycan profile changes as a potential biomarker for mouse aging. As kl/kl mice die between 8 and 10 weeks of age, serum samples from kl/kl mice and controls of the same genetic background were obtained at the age of 7 weeks and studied for *N*-glycan profiles. Peak 1 and peak 6 in the kl/kl mice were significantly higher compared to the controls, whereas no significant change in peak 5 was observed (Fig. 4D–F).

To study whether *Fut8* gene expression is correlated with the changes in glycosylations in dw/dw and kl/kl mice, we analyzed gene expression in the livers using Q-PCR. Liver RNA was prepared from 6-month-old dw/dw mice (n = 6, males) and age- and sex-matched controls (n = 6, males), as well as from 7-week-old kl/kl (n = 5, males) and age- and sex-matched controls (n = 5, males). In correlation with the glycan structures, *Fut8* gene expression in dw/dw mice was decreased (Fig. 5A), whereas

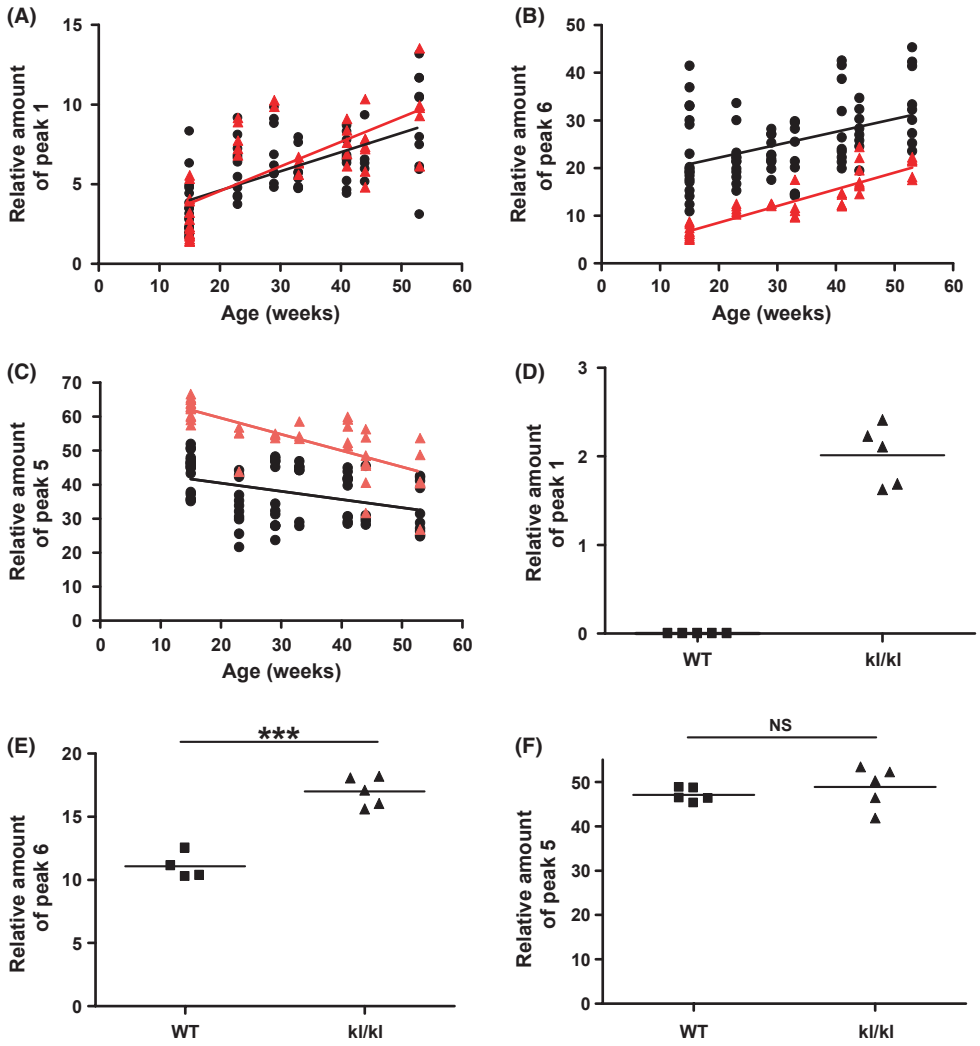

Fig. 4 (A–C) N-glycosylation alterations in serum proteins of dw/dw mice (n = 10) and age- and background-matched controls (n = 10, WT). (D–F) N-glycosylation alterations in serum proteins of kl/kl mice (n = 5) and age- and background-matched controls (n = 5, WT) at 7 weeks of age. (A–C) The area under the peaks that represents the relative concentrations of the oligosaccharide structures (in percentage) was analyzed statistically for correlation between *N*-glycan and genotype. Blood was taken longitudinally throughout the lifespan. The WT group is presented by the black line and dots and the dw/dw group by the red line and triangles. (A) There is an age-dependent increase of peak 1 in both groups (WT r = 0.6185, P < 0.0001 and dw/dw = 0.7167, P < 0.0001). There is no significant difference between the slopes of the WT and dw/dw. (B) There is an age-dependent increase in peak 6 with age in both conditions over the lifespan analyzed here (WT r = 0.4364, P < 0.0001 and dw/dw r = 0.8936, P < 0.0001). Although the amount of peak 6 is higher throughout the lifespan in WT compared with dw/dw, there is no significant difference between the slope of WT and dw/dw mice. (C) There is an age-dependent decrease in peak 5 with age in both conditions over the lifespan analyzed here (WT r = −0.3803, P = 0.0009 and dw/dw r = −0.7419, P < 0.0001). The amount of peak 5 is throughout the lifespan higher in WT compared to dw/dw. There is no significant difference between the slope of WT and dw/dw mice. (D–F) The area under the peaks that represents the relative concentrations of the oligosaccharide structures (in percentage) was analyzed statistically for correlation between glycan and genotype. (D) The relative amount of peak 1 in WT mice was below the detection limit and was determined as 0; therefore, no statistical test could be performed on these data but there is a clear trend of increased peak 1 in the kl/kl mice. (E) Statistically significant increase of peak 6 in kl/kl mice. (F) Not statistically significant (NS) difference of relative amount of peak 5 in function of the genotype.

Fut8 expression in kl/kl mice was increased (Fig. 5B). Also, the FUT8 biological activity followed the same trend confirming the gene expression effect is visible in FUT8 biological activity (Fig. 5C,D).

Influence of FUT8 on IGF-1 signaling pathway

Fucosylation can affect several signaling pathways. An important example is the epidermal growth factor receptor (EGFR) that needs core-α-1,6-fucosylation for correct signaling as FUT8$^{-/-}$ cells have reduced EGF signaling (Wang *et al.*, 2006b). As FUT8 is upregulated during aging, we investigated how altered *Fut8* expression influences IGF-1 signaling.

First, we used primary hepatocytes isolated from young (low *Fut8* expression) and old (high *Fut8* expression) mice. These cells were stimulated with 400 ng mL^{-1} IGF-1 after overnight starvation, and IGF-1Rβ phosphorylation was measured using a phospho-specific antibody against P-IGF-1Rβ. It is clear that at all time points, P-IGF-1Rβ bands are less intense in young hepatocytes compared to old hepatocytes (Fig. 6A, upper panel), although the total levels of IGF-1Rβ were the same (Fig. 6A, fifth panel) demonstrating that the activation and sensitivity of the IGF-1R signaling pathway increased in old hepatocytes compared to young hepatocytes. The reason for this can be altered N-glycosylation. To test this hypothesis, we performed similar experiments, but first pretreated

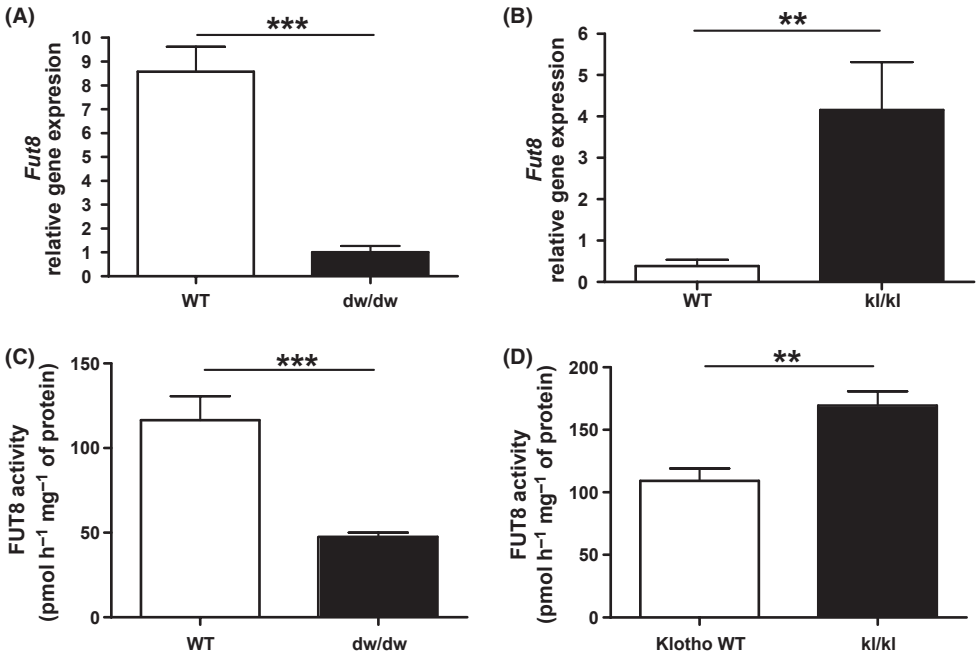

Fig. 5 The relative gene expression and activity of FUT8 in the liver of dw/dw, kl/kl and their corresponding WT mice. (A) Decreased expression of *Fut8* in 6-month-old dw/dw mice (n = 10) compared with age- and strain-matched controls (WT, n = 10) measured by Q-PCR. (B) Increased expression of *Fut8* in 7-week-old kl/kl mice (n = 5) compared to age- and strain-matched controls (WT, n = 5) measured by Q-PCR. (C) Decreased activity of FUT8 in 6-month-old dw/dw mice (n = 6) compared to age- and strain-matched controls (WT, n = 6). (D) Increased activity of FUT8 in 7-week-old kl/kl mice (n = 4) compared to age- and strain-matched controls (WT, n = 4).

the cells for 48 h with tunicamycin. Tunicamycin is an inhibitor of the N-glycosylation biosynthesis pathway. In tunicamycin-pretreated cells, the difference in the intensity of P-IGF-1Rβ bands in young vs. old hepatocytes is almost totally abolished (Fig. 6A third panel), confirming that *N*-glycosylation indeed could play a role in the IGF-1R signaling pathway. To study whether the difference in phosphorylation of the IGF-1R really influences downstream events, the same young and old hepatocytes were stimulated with IGF-1, and as a readout of the IGF-1 pathway, lipid synthesis was analyzed. Indeed, IGF-1 is known to increase lipid synthesis very significantly (Makrantonaki *et al.*, 2008). Both 48 and 72 h after IGF-1 stimulation, we observed that hepatocytes derived from old mice (23 months of age), with higher *Fut8* expression, respond significantly better to IGF-1 compared to hepatocytes isolated from young mice (5 months of age; Fig. 6B and supplemental Fig. S2A).

As there might be much more differences between old and young hepatocytes than *Fut8* expression, we engineered a stable cell line with reduced *Fut8* expression. We used sebocytes as these cells are known to have a good functioning IGF-1 pathway (Makrantonaki *et al.*, 2008). By lentiviral transfection of *Fut8* siRNA, we specifically downregulated *Fut8* in the sebocytes and found in these cells a significant reduction in *Fut8* gene expression (supplemental Fig. S1A), protein level (supplemental Fig. S1B), and consequently cell-bound α-1,6-core fucosylation (supplemental Fig. S1C) compared to the control cell line. Stimulation of FUT8 KD sebocytes with IGF-1 demonstrated less intense P-IGF-1Rβ bands compared to the controls sebocytes (Fig. 6C top panel), while no difference was found in total IGF-1Rβ bands (Fig. 6C third panel). Although the difference in intensity of P-IGF-1Rβ bands is subtle, they are very reproducible and sufficient enough to alter downstream events such as IGF-1-induced lipid synthesis (Fig. 6D and supplemental Fig. S2B). These data confirm that *Fut8* expression levels possibly play a role in signaling of the IGF-1 receptor pathway.

Discussion

We previously showed that three major *N*-glycan structures present in human blood glycoproteins are altered with age (Vanhooren *et al.*, 2007, 2010). Here, we investigated the possibility that age-related N-glycosylation changes occur also in mice. It is particularly important to know whether N-glycosylation changes are specific for human aging or rather a general aspect of aging in different mammalian species. Also, because we can follow genetically identical mice in SFP conditions, we can study whether these age-related N-glycosylation alterations are inbedded in the genome or are owing to the environmental effects or genetic polymorphisms. *N*-glycan profiles in mouse serum were somewhat different from those in human serum, reflecting some species-specific differences in *N*-glycan structures. We found that three structures were aging related: the relative serum levels of NGA2F (peak 1) and NA2F (peak 6) increased with age while NA2 (peak 5) decreased, demonstrating that N-glycosylation of serum proteins is altered during mouse aging. Because age-related N-glycosylation changes also occur in genetically identical inbred mice, kept in a constant SPF environment, we can conclude that these changes are rather encoded in the genome of mice, and we can speculate that this could also be the case in humans as they also demonstrate age-related N-glycosylation changes. To confirm the origin of human age-related N-glycosylation alterations, we should study genetically identical humans during their entire lifespan, protected from any environmental stimuli, which is impossible. An alternative could be to study the N-glycosylation changes during the lifespan of genetically identical twins living in a similar environment. There are some twins databases, e.g. Italian Twin Registry (Fagnani *et al.*, 2006) and the Danish Twin Registry (Skytthe *et al.*, 2006), which could make this work possible.

To validate the N-glycosylation changes in healthy mouse aging and to study whether intervention in the aging process can alter these changes,

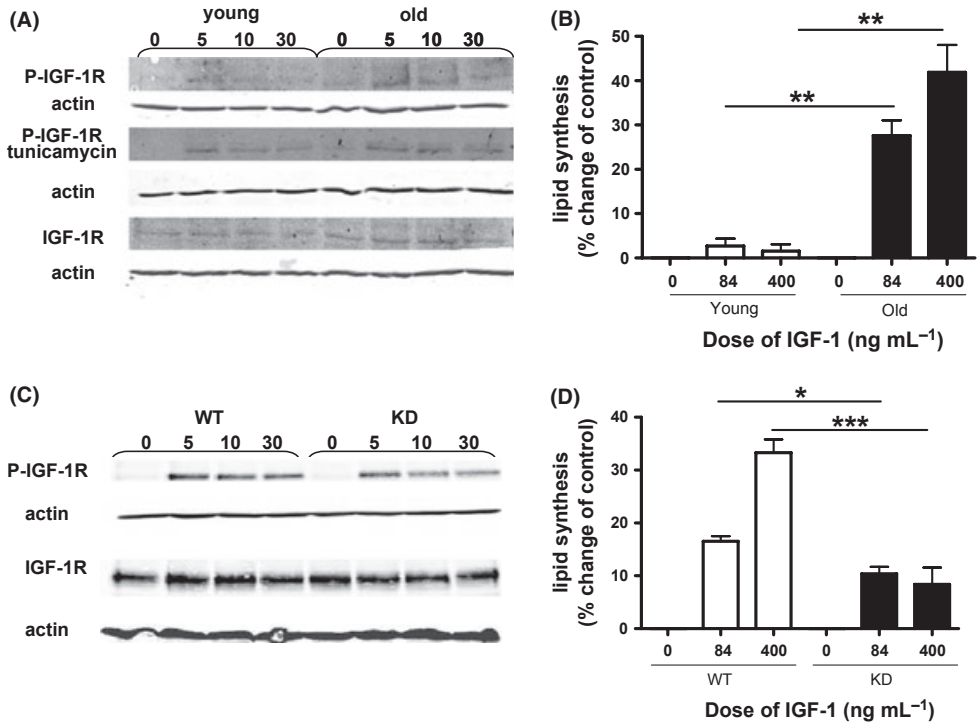

Fig. 6 IGF-1 induced phosphorylation of the IGF-1Rβ and downstream IGF-1 induced lipid synthesis. (A) Hepatocytes isolated from young (5 months, left lanes 1–4) and old (23 months, right lanes 5–8) male C57BL/6 mice were stimulated with 400 ng mL^{-1} IGF-1 for 5, 10, and 30 min after overnight starvation. Western blots for P-IGF-1Rβ (top panel), P-IGF-1Rβ after 48-h tunicamycin incubation (third panel), total IGF-1Rβ (fifth panel), with corresponding actin control (panels two, four, and six). Less activation of the IGF-1Rβ is observed in the young vs. old hepatocytes, and this difference is almost completely abolished by tunicamycin treatment. (B) Hepatocytes isolated from young (5 months, white bars) and old (23 months, black bars) male C57BL/6 mice were stimulated with 0, 84, or 400 ng mL^{-1} mouse IGF-1 for 72 h. The lipid induction was measured with Nile red. A significant increased lipid synthesis was observed in the old hepatocytes compared with the young hepatocytes. (C) Control sebocytes (left lanes 1–4) and FUT8 KD sebocytes (right lanes 5–8) were stimulated with 400 ng mL^{-1} IGF-1 for 5, 10, and 30 min after overnight starvation. Western blots for P-IGF-1Rβ (top panel), and total IGF-1Rβ (third panel), with corresponding actin controls (panel two and four). Less activation of the IGF-1Rβ is observed in the KD cells compared to the control cells. (D) Control (white bars) and FUT8 KD (black bars) sebocytes were stimulated with 0, 84, or 400 ng mL^{-1} human IGF-1 for 72 h (B). The lipid induction was measured with Nile red. A significant decreased lipid synthesis was observed in the KD sebocytes compared to the control sebocytes.

making N-glycosylation a good biomarker for physiological age, we studied mice subjected to dietary intervention (CR). It has been known for many years that CR can retard the aging process (Weindruch *et al.*, 1988). Indeed, we demonstrated an inversion in the age-related changes in the *N*-glycan structures, indicating that CR has an effect on N-glycosylation of serum proteins. This is particularly interesting for the study of CR mimetics. Many research groups and companies are searching for components that can mimic CR intervention (Ingram *et al.*, 2006; Smith *et al.*, 2010). Using mice and N-glycosylation as a biomarker of physiological age, already early in the treatment, an idea can be formed if the component is working. To further study the correlation between N-glycosylation and aging and to find hints about the mechanism behind age-related N-glycosylation changes, we used mice with an extended or shortened lifespan, namely two genetically manipulated mouse models: dw/dw mice (extended lifespan) and kl/kl mice (shortened lifespan). These mice have proven to be very valuable tools for aging research but it has to be stressed that dw/dw as well as kl/kl mice are just 'models' of the aging process and do not mimic slower or faster aging in all aspects (Matsushima *et al.*, 1986; Razzaque & Lanske, 2006). In dw/dw mice, which have an extended lifespan, the age-related glycosylation changes of peak 5 and peak 6 were delayed compared to controls. The fact that the slope in dw/dw is not different compared to the WT mice is interesting. It confirms that the dw/dw mice are aging too but the fact that their fucosylation levels are always lower than the WT gives the impression that it will take them longer to reach a 'fatal' fucosylation threshold and therefore live longer. No differences are seen in the levels of peak 1 in WT vs. dw/dw, which could be a reflection of the limits of the dw/dw model or could mean that peak 1 is differently regulated than peaks 5 and 6. kl/kl mice have a greatly shorted lifespan and demonstrate premature aging symptoms (klotho also regulates IGF-1 signaling), although some of these phenotypes can be rescued by vitamin D-deficient diets (Razzaque & Lanske, 2006). kl/kl mice exhibit an N-glycosylation profile resembling that of much older wild-type mice except for peak 5. The reason for a stable peak 5 is probably because the time frame of sampling is very short because of the extremely short lifespan: these mice die very fast (< 10 weeks of age); therefore, only 1 time point could be studied, which somewhat limits the extrapolation of the results.

One general aspect which is consistent in all four different mouse groups studied (SPF normal aging mice, CR, dw/dw and kl/kl mice) is the age-related change in peak 6, which makes it an interesting molecular pathway to study in-depth. *N*-glycan precursors are synthesized in the ER and Golgi by the subsequent addition of GlcNAc, Gal, and fucose molecules by the corresponding oligosaccharyltransferases; also, glycosidases play a role in modeling of the *N*-glycans (Ohtsubo & Marth, 2006; Varki *et al.*, 2009). Changes in the *N*-glycan profile in serum are likely to be related to changes in the expression levels of glycosyltransferases in liver cells, which would lead to modifications in both core and terminal structures of glycans. Indeed, we observed alteration during normal mouse aging in the expression of the α-1,6-fucosyltransferase (*Fut8*) gene, which is the only fucosyltransferase involved in core-fucosylation in mice (Varki

et al., 2009). Thus, the increase of core-fucosylated peak 1 (NGA2F) and peak 6 (NA2F) during mouse aging could be at least partly owing to an increase in *Fut8* gene expression. Consequently, altered expression of *Fut8* could lead to changes in the level of peak 5 (NA2), which is a substrate for FUT8. The significant correlation between the levels of *Fut8* gene expression and *N*-glycan (peak 6) was confirmed in long-living CR and dw/dw Dwarf mice as well as in the short living kl/kl mice. In agreement, FUT8 activity measured in the livers of aging C57BL/6 mice, dw/dw, and kl/kl mice was also correlated with the gene expression data and with age. FUT8 is known to play a key role in regulating physiological functions by modifying functional proteins to induce changes in TGF-β signaling, EGFR-mediated signaling, integrin α3β1-mediated cell adhesion, and VEGFR-2 expression (Wang *et al.*, 2005, 2006a,b, 2009; Kondo *et al.*, 2006; Zhao *et al.*, 2006). Upregulation of FUT8 could have enormous effects on different signaling pathways and could thus influence the aging process. Therefore, we investigated what the influence of FUT8 expression is on the IGF-1 signaling pathway, as IGF-1 is strongly linked with aging in mammals (Russell & Kahn, 2007). Another reason for studying the IGF-1R signaling pathways is that in all 3 mouse models studied (CR, dw/dw and kl/kl mice), next to peak 6 levels, also serum IGF-1 levels are correlated with the lifespan; in CR and dw/dw mice, IGF-1 and peak 6 levels are lower while lifespan is longer, and in kl/kl mice, IGF-1 and peak 6 levels are higher and lifespan is shorter. Using hepatocytes from old and young mice, we could demonstrate that old hepatocytes, with increased *Fut8* expression, have a more sensitive IGF-1R signaling pathway. As the difference between old and young hepatocytes goes beyond *Fut8* expression, we engineered a stable sebocyte cellline with reduced *Fut8* expression. By reducing *Fut8* in these cells, the IGF-1 signaling is reduced.

The increased *Fut8* expression during aging could make the IGF-1 signaling pathway more sensitive in an older organism. In our view, although the levels of IGF-1 itself drop during aging (Toogood *et al.*, 1996), the receptor becomes more sensitive by core fucosylation. As the IGF-1R is more sensitive in an old organism, lower amounts of IGF-1 could still activate the IGF-1R, thereby inhibiting further downstream FOXO to translocate to the nucleus, in turn inhibiting the expression of 'longevity genes' (e.g. antioxidants) and favoring the expression of pro-aging genes (Russell & Kahn, 2007). Future research should demonstrate whether the age-related FUT8 increase influences the IGF-1R by increasing core fucosylation of the IGF-1R itself or by modulating other molecules that influence the IGF-1 pathway. As it is already known that changes in *Fut8* expression levels influence the fucosylation state of the EGFR (Wang *et al.*, 2006b), this could be the cause of altered IGF-1 signaling as it is shown that EGFR regulates the stability of the IGF-1R (Riedemann *et al.*, 2007).

To confirm that FUT8 is really modulating the aging process by itself and to justify that a search for FUT8 inhibitors might make sense in the treatment for aging, it would be interesting to knock down FUT8 expression *in vivo* in mature mice and follow their lifespan. Full FUT8 KO mice die soon after birth as FUT8 is extremely important during postnatal development (Wang *et al.*, 2006b), which is reflected by the high *Fut8* expression in wild-type mice during the first 8 weeks after birth. In adult mice, the *Fut8* expression drops to a very low minimum and slowly rises again during aging (our findings, Bakkers *et al.*, 1997; Miyoshi *et al.*, 1997). Generating a conditional FUT8 KO, where FUT8 can be knocked out for example in the liver, could be considered, but such a knockout will probably cause physiological problems as some *Fut8* expression will always be needed to some extend for basic physiological processes. Therefore, it would be interesting to knockdown *Fut8* expression in mature mice by shRNA, for example in the liver, thereby reducing but not fully abolishing *Fut8* expression, and follow the lifespan of these mice.

In conclusion, our results demonstrate that the *N*-glycan age-related dynamics are indeed associated with aging and that they could be developed into a convenient biomarker of mouse aging to monitor physiological age and to follow the effects of antiaging interventions, for instance, monitoring the effects of CR mimetics and antiaging medicines. We also discovered that increased expression and activity of FUT8 in the liver are strongly linked to the age-related changes in glycosylation and that this increased FUT8 and fucosylation influence IGF-1 signaling.

Materials and methods

C57BL/6 Mice

C57BL/6 mice were purchased from Elevage *Janvier* (Le-Genest-Saint-Ile, France). The mice were housed in a SPF animal facility. They were maintained in a temperature-controlled, air-conditioned environment with 14- to 10-h light/dark cycles, and they received food and water *ad libitum*, except mice on a CR diet, which were fed a diet with 40% less calories. Blood samples were collected from the tail vein every month. The blood was allowed to clot 30 min at 37°C and overnight at 4°C, and serum was obtained by centrifugation at 20 000 *g* for 10 min and stored at –20°C. Mice were sacrificed by cervical dislocation at different time points. Organs were flushed and dissected out. All experiments were approved by the local ethics committee.

CR mice

C57BL/6 mice (n = 8) were fed a diet containing 40% less calories than the control group (n = 8) starting at the age of 2 months. They were maintained on this diet for 6 months. Blood samples were collected from the tail vein every month.

Snell Dwarf mice

Serum and liver samples of dw/dw homozygous and controls (DW/J × C3H/HeJ) F2 animals aged 6 month were kindly provided by Prof. Dr. R. Miller (Michigan, USA). To follow these mice during their life span, male dw/dw homozygous mice (n = 10) and control WT littermates (n = 10) were purchased from the Jackson Laboratories (Maine, USA). The mice were housed as described previously, and the blood samples were collected from the tail vein every month.

kl/kl mice

A congenic strain of the kl/kl mice was established by backcrossing the original kl/+ mice (Kuro-o *et al.*, 1997) to 129S1SvImJ mice for nine generations and used for this study. Serum and liver samples from kl/kl and control male mice were obtained at 7 weeks of age.

N-glycan analysis using the ABI 3130 sequencer

To analyze the N-glycosylation structures on mouse serum *N*-glycoproteins, DSA-FACE was used as described previously (Vanhooren *et al.*, 2008).

AOL lectin blot

Control sebocytes and FUT8 KD sebocytes were lysed with Disc lysis buffer (30 mM Tris–HCl pH 7.5, 150 mM NaCl, 1% Triton-X100, 10% glycerol, protein inhibitor cocktail; Roche, Vilvoorde, Belgium). Normal serum

(generated as described in Material and Methods *C57BL/6*) was used for the AOL lectin blot (Fig. 2). Protein concentration was measured with BCA protein Assay kit (Pierce, Rockford, IL, USA). 50 μg (for the sebocytes) and 35 μg (for serum) of proteins were separated by electrophoresis in 10% sodium dodecyl sulfate–polyacrylamide gel. The proteins were then transferred to a nitrocellulose membrane for lectin blot analysis. The membranes were blocked overnight at 4°C with 3% bovine serum albumin (BSA) in Tris-buffered saline (150 mM NaCl, 50 mM Tris–HCl pH 7,4, and TBS) and incubated for 1 h at room temperature with biotinylated Aspergillus oryzae L-fucose-specific lectin (AOL) (Funakoshi Co., Ltd., Tokyo, Japan) (5 mg mL^{-1}, 1:400) in TBST (TBS containing 0.05% Tween 20). After four washes of 5 min each with TBST, the membranes were blocked in 5% milk-TBS for 1 h, incubated with Streptavidin Alexa Fluor 647 (1:2000) for 1 h at room temperature in 3% milk-TBS containing 0.1% Tween. The membranes were washed four times with TBS containing 0.1% Tween and finally with TBS. For normalization, immunoreaction with mouse anti-actin (1:10000; MP Biomedicals, Illkirch Cedex, France) as primary antibody and goat anti-mouse IRDye 680 (1:15000; Li-Cor, Westburg, Leusden, The Netherlands) as secondary antibody was performed. Blot was scanned at 680 nm using Odyssey Imager. As a control, the same samples were also separated by electrophoresis in 10% sodium dodecyl sulfate–polyacrylamide gel and the gel was stained for total protein with coomassie for 1 h and destained overnight.

Isolation of liver hepatocytes

The isolation relied on a two-step procedure, including *in situ* perfusion/digestion of the liver and purification based on cell density but without using pronase digestion. Hepatocytes were isolated from male C57BL/6 mice. Subsequently, liver digest medium was applied for enzymatic digestion of the tissue at 37°C, which was supplemented with Collagenase P (0.025% m/v; Roche Diagnostics, Mannheim, Germany). After digestion, the tissue was manually disrupted and filtered into medium containing Collagenase P (0,05% m/v) and Dnase I (Roche Diagnostics). The resulting cell suspension was filtered through a sieve and centrifuged two times at 50 *g* for 2 min. The pellet was resuspended with 24 mL of DMEM 10% FCS. Then, hepatocyte enrichment relied on a centrifugation, 750 *g* for 20 min, through a three-layer discontinuous Percoll gradient (Amersham Biosciences, Ghent, Belgium) (Goncalves *et al.*, 2007). An aliquot of the cell preparation was separated for cell count and viability analysis (light microscopy and trypan blue exclusion test). One million of hepatocytes per well were placed on rat tail collagen-1-coated well plates in hepatocyte basal medium with 10% FCS. After 4 h, the medium was changed to a medium without FCS, and hepatocytes were used immediately for further investigations.

Western blot analysis of IGF-1 stimulated cells

Young/old hepatocytes and FUT8 control and FUT8 knockdown sebocytes were stimulated with 400 ng mL^{-1} during 5, 10, and 30 min after overnight starvation. In some experiments, the hepatocytes were first incubated with 1 μg mL^{-1} tunicamycin (Sigma, Bornem, Belgium) for 48 h prior to IGF-1 stimulation. After stimulation, the cells were washed and lysed in lysis buffer containing protein inhibitor cocktail (Roche Diagnostics, Vilvoorde, Belgium) and phosphatase inhibitors (Phosstop tablets; Roche Diagnostics and calyculin a, MP Biomedicals, LLC, Europe). Protein concentration was measured with BCA protein Assay kit (Pierce). Fifty microgram of proteins was separated by electrophoresis in 10% sodium dodecyl sulfate–polyacrylamide gel. The proteins were then transferred to a nitrocellulose membrane for Western blot analysis. The membranes were blocked 1 h at RT with 5% BSA in Tris-buffered saline (150 mM NaCl, 50 mM Tris–HCl pH 7,4, TBS) and then incubated with an antibody against the phosphorylated form of the IGF-1Rβ (phosphorylated at tyrosine 1135/1136, 1:1000 rabbit anti-P-IGF-1Rβ; Cell Signaling, Beverly, MA, USA) in 5% BSA, 1× TBS, 0.1% Tween-20 overnight at 4°C. The same was carried out with an antibody that detects total IGF-1Rβ levels, independently of the phosphorylation state (1:1000 rabbit anti-IGF-1R β; Cell Signaling). The blots were also probed with actin (1:10000 mouse anti-actin; MP Biomedicals LLC) for normalization. As a secondary antibody for IGF-1Rβ and P-IGF-1Rβ, an anti-rabbit IRDye 800 (1:15000; Li-Cor) was used. As a secondary antibody for actin, an anti-mouse IRDye 800 (1:15000; Li-Cor) was used. Blots were scanned at 680 and 800 nm using Odyssey Imager.

Lipid synthesis test

Hepatocytes were isolated from young mice (5 months old) and old mice (23 months old) as described earlier. They were seeded out in 96-well fluorescence plates at 20000 cells per well and starved overnight. Control and KD sebocytes were also seeded out in 96-well fluorescence plates at 20 000 cells per well and starved overnight. The following day mouse (for hepatocytes) or human (for sebocytes) recombinant IGF-1 (Sigma) was added at concentrations of 0, 84, and 400 ng mL^{-1} (each condition in eightfold). Lipid assay was performed after 48 and 72 h of IGF-1 stimulation. Every day, medium was replaced with fresh medium with IGF-1 (without IGF-1 for the 0 ng mL^{-1} condition). For lipid detection, cells were washed twice with PBS, and 100 μL of a 10 μg mL^{-1} Nile red (Sigma) solution in PBS was added to each well. The plates were then incubated at 37°C for 30 min, and the released fluorescence was measured with a Fluostar Optima (bMG) spectrofluorimeter. The result was presented as percentages of the absolute fluorescence units in comparison with the controls, using 485-nm excitation and 520-nm emission filters for neutral lipids.

RNA, cDNA, and qPCR

Approximately 30 mg of frozen liver tissue was ground in liquid nitrogen, and RNA was prepared with the RNeasy Mini kit (Qiagen Benelux B.V., Venlo, the Netherlands). Sebocytes were grown in a 6-well plate, 600 μL RLT lysis buffer was added, the lysate was passed 5 times through a 20-gauge needle (0.9 mm diameter), and RNA was further prepared with the RNeasy Mini kit (Qiagen Benelux B.V.). DNase digestion was performed with the RNase-free DNase Set of Qiagen. cDNA synthesis was performed with the iScript cDNA synthesis kit of Bio-Rad starting from 2 μg of total RNA. Real-time qPCR using the Light Cycler 480 (Roche Diagnostics) was performed with a fivefold dilution of the cDNA. Each 10-μL assay contained 5 μL of 2× Fast SYBR Green Master Mix (Applied Biosystems, Nieuwerkerk Ad Ijssel, The Netherlands), 2 μL primer mix for each gene (0.5 μM each final concentration), and 3 μL of diluted cDNA. The primers were designed with the PrimerExpress software or selected from the Primerbank of Harvard. A geometric averaging method (GeNorm) identified the two best housekeeping genes among the eight examined (Actb, Gapd, B2m, Tbp, Hprt1, Rn18s, RPL13a.1, and Ubc). Each reaction was performed in triplicate. PCR cycling consisted of denaturation at 95°C for 5 min, 50 cycles of 95°C for 10 s and 60°C for 30 s, and detection for 1 s at 72°C. The Ct data were analyzed using Excel and GraphPad Prism 4.

Primers sequences used were as follows: Mouse FUT8-forw: CAGGGGATTGGCGTGAAAAAG, Mouse FUT8-rev: CGTGATGGAGTTGACAACCATAG, Human FUT8-forw: CCTGGCGTTGGATTATGCTCA, Human FUT8-reve: GACAGTTCTCGGCTAGAGTGA.

FUT8 activity assay

Mice livers were homogenized with a Potter-Elvehjem homogenizer in three volumes of 10 mM Tris–HCl buffer (pH 7.4), 0.25 M sucrose, supplemented with a protease inhibitor cocktail (Complete EDTA-free; Roche). After centrifugation at 600 *g* for 5 min at 4°C, the supernatants were collected and used as the crude enzyme preparations for FUT8 activity assay. FUT8 activity was assayed according to the method of Ihara *et al.* (2006), with minor modifications. The standard assay mixture contained the following components in a volume of 10 μL: 100 mM MES-NaOH buffer (pH 7,0), 0,5% Triton X-100, 0.5 mM GDP-β-L-fucose, 10 μM GnGnbi-Asn-PNSNB, 200 mM GlcNAc, 1 mg mL^{-1} BSA, and the crude enzyme extract (3 μL). After incubation at 37°C for 2 h, 40 μL of water was added, and the reaction was terminated by boiling for 3 min. After centrifugation at 20 000 *g* for 5 min, 10 μL of the supernatant was injected in an HPLC equipped with a TSK gel ODS-80TM column (0.46 × 15 cm; Tosoh, Tokyo, Japan) to separate and measure the product. Elution was performed at 55°C using 20 mM ammonium acetate buffer (pH 4.0) containing 0.15% 1-butanol at a flow rate of 1 mL min^{-1}. The protein concentration was determined with a BCA protein assay reagent (Pierce) using BSA as the standard.

Statistical analysis

Mean values were compared using an unpaired Student's t-test. Correlations were analyzed by Pearson test when the data were normally distributed. Data are presented as mean ± standard error. Significance levels are as follows: $*0.01 \le P < 0.05$, $**0.001 \le P < 0.01$, and $***P < 0.001$.

Acknowledgments

We thank Dr Amin Bredan for editing the manuscript. This work was supported by a grant from Ghent University (BOF No. 01106205), Flanders-China Bilateral project (011S605), the FWO and BELSPO (IUAP-VI/18).

References

Andressoo JO, Hoeijmakers JH (2005) Transcription-coupled repair and premature ageing. *Mutat. Res.* **577**, 179–194.

Bakkers J, Semino CE, Stroband H, Kijne JW, Robbins PW, Spaink HP (1997) An important developmental role for oligosaccharides during early embryogenesis of cyprinid fish. *Proc. Natl Acad. Sci. USA* **94**, 7982–7986.

Bielschowsky F, Bielschowsky M (1959) Carcinogenesis in the pituitary dwarf mouse. The response to methylcholanthrene injected subcutaneously. *Br. J. Cancer* **13**, 302–305.

Fagnani C, Brescianini S, Cotichini R, D'Ippolito C, Dukic T, Giannantonio L, Medda E, Nistico L, Patriarca V, Pulciani S, Rotondi D, Toccaceli V, Stazi MA (2006) The Italian Twin Register: new cohorts and tools, current projects and future perspectives of a developing resource. *Twin Res. Hum. Genet.* **9**, 799–805.

Flurkey K, Papaconstantinou J, Miller RA, Harrison DE (2001) Lifespan extension and delayed immune and collagen aging in mutant mice with defects in growth hormone production. *Proc. Natl Acad. Sci. USA* **98**, 6736–6741.

Flurkey K, Papaconstantinou J, Harrison DE (2002) The Snell dwarf mutation Pit1(dw) can increase life span in mice. *Mech. Ageing Dev.* **123**, 121–130.

Freeze HH, Aebi M (2005) Altered glycan structures: the molecular basis of congenital disorders of glycosylation. *Curr. Opin. Struct. Biol.* **15**, 490–498.

Goncalves LA, Vigario AM, Penha-Goncalves C (2007) Improved isolation of murine hepatocytes for in vitro malaria liver stage studies. *Malar. J.* **6**, 169.

Ihara H, Ikeda Y, Taniguchi N (2006). Reaction mechanism and substrate specificity for nucleotide sugar of mammalian alpha1,6-fucosyltransferase – a large-scale preparation and characterization of recombinant human FUT8. *Glycobiology* **16**, 333–342.

Ingram DK, Zhu M, Mamczarz J, Zou S, Lane MA, Roth GS, deCabo R (2006) Calorie restriction mimetics: an emerging research field. *Aging Cell* **5**, 97–108.

Kondo A, Li W, Nakagawa T, Nakano M, Koyama N, Wang X, Gu J, Miyoshi E, Taniguchi N (2006) From glycomics to functional glycomics of sugar chains: identification of target proteins with functional changes using gene targeting mice and knock down cells of FUT8 as examples. *Biochim. Biophys. Acta* **1764**, 1881–1889.

Kukuruzinska MA, Lennon K (1998) Protein N-glycosylation: molecular genetics and functional significance. *Crit. Rev. Oral Biol. Med.* **9**, 415–448.

Kuro-o M, Matsumura Y, Aizawa H, Kawaguchi H, Suga T, Utsugi T, Ohyama Y, Kurabayashi M, Kaname T, Kume E, Iwasaki H, Iida A, Shiraki-Iida T, Nishikawa S, Nagai R, Nabeshima YI (1997) Mutation of the mouse klotho gene leads to a syndrome resembling ageing. *Nature* **390**, 45–51.

Lautenschlager NT, Almeida OP (2006) Physical activity and cognition in old age. *Curr. Opin. Psychiatry* **19**, 190–193.

Li S, Crenshaw EB 3rd, Rawson EJ, Simmons DM, Swanson LW, Rosenfeld MG (1990) Dwarf locus mutants lacking three pituitary cell types result from mutations in the POU-domain gene pit-1. *Nature* **347**, 528–533.

Liu XE, Dewaele S, Vanhooren V, Fan YD, Wang L, Van Huysse J, Zhuang H, Contreras R, Libert C, Chen CC (2010) Alteration of N-glycome in diethylnitrosamine-induced hepatocellular carcinoma mice: a non-invasive monitoring tool for liver cancer. *Liver Int.* **30**, 1221–1228.

Lombard DB, Chua KF, Mostoslavsky R, Franco S, Gostissa M, Alt FW (2005) DNA repair, genome stability, and aging. *Cell* **120**, 497–512.

Makrantonaki E, Vogel K, Fimmel S, Oeff M, Seltmann H, Zouboulis CC (2008) Interplay of IGF-I and 17beta-estradiol at age-specific levels in human sebocytes and fibroblasts in vitro. *Exp. Gerontol.* **43**, 939–946.

Mariani E, Polidori MC, Cherubini A, Mecocci P (2005) Oxidative stress in brain aging, neurodegenerative and vascular diseases: an overview. *J. Chromatogr. B Analyt. Technol. Biomed. Life Sci.* **827**, 65–75.

Matsumura K, Higashida K, Ishida H, Hata Y, Yamamoto K, Shigeta M, Mizuno-Horikawa Y, Wang X, Miyoshi E, Gu J, Taniguchi N (2007) Carbohydrate binding specificity of a fucose-specific lectin from Aspergillus oryzae: a novel probe for core fucose. *J. Biol. Chem.* **282**, 15700–15708.

Matsushima M, Kuroda K, Shirai M, Ando K, Sugisaki T, Noguchi T (1986) Spermatogenesis in Snell dwarf, little and congenitally hypothyroid mice. *Int. J. Androl.* **9**, 132–140.

Miyoshi E, Uozumi N, Noda K, Hayashi N, Hori M, Taniguchi N (1997) Expression of alpha1-6 fucosyltransferase in rat tissues and human cancer cell lines. *Int. J. Cancer* **72**, 1117–1121.

Ohtsubo K, Marth JD (2006) Glycosylation in cellular mechanisms of health and disease. *Cell* **126**, 855–867.

Parekh R, Roitt I, Isenberg D, Dwek R, Rademacher T (1988) Age-related galactosylation of the N-linked oligosaccharides of human serum IgG. *J. Exp. Med.* **167**, 1731–1736.

Raman R, Raguram S, Venkataraman G, Paulson JC, Sasisekharan R (2005) Glycomics: an integrated systems approach to structure-function relationships of glycans. *Nat. Methods* **2**, 817–824.

Razzaque MS, Lanske B (2006) Hypervitaminosis D and premature aging: lessons learned from Fgf23 and Klotho mutant mice. *Trends Mol. Med.* **12**, 298–305.

Rennels EG, Anigstein DM, Anigstein L (1965) A cumulative study of the growth of sarcoma 180 in anterior pituitary dwarf mice. *Tex. Rep. Biol. Med.* **23**, 776–781.

Riedemann J, Takiguchi M, Sohail M, Macaulay VM (2007) The EGF receptor interacts with the type 1 IGF receptor and regulates its stability. *Biochem. Biophys. Res. Commun.* **355**, 707–714.

Russell SJ, Kahn CR (2007) Endocrine regulation of ageing. *Nat. Rev. Mol. Cell Biol.* **8**, 681–691.

Skytthe A, Kyvik K, Bathum L, Holm N, Vaupel JW, Christensen K (2006) The Danish Twin Registry in the new millennium. *Twin Res. Hum. Genet.* **9**, 763–771.

Smith DL Jr, Nagy TR, Allison DB (2010) Calorie restriction: what recent results suggest for the future of ageing research. *Eur. J. Clin. Invest.* **40**, 440–450.

Toogood AA, O'Neill PA, Shalet SM (1996) Beyond the somatopause: growth hormone deficiency in adults over the age of 60 years. *J. Clin. Endocrinol. Metab.* **81**, 460–465.

Vanhooren V, Desmyter L, Liu XE, Cardelli M, Franceschi C, Federico A, Libert C, Laroy W, Dewaele S, Contreras R, Laroy W, Dewaele S, Contreras R, Chen C (2007) N-glycomic changes in serum proteins during human aging. *Rejuvenation Res.* **10**, 521–531a.

Vanhooren V, Laroy W, Libert C, Chen C (2008) N-glycan profiling in the study of human aging. *Biogerontology* **9**, 351–356.

Vanhooren V, Dewaele S, Libert C, Engelborghs S, De Deyn PP, Toussaint O, Debacq-Chainiaux F, Poulain M, Glupczynski Y, Franceschi C, Jaspers K, van der Pluijm I, Hoeijmakers J, Chen CC (2010) Serum N-glycan profile shift during human ageing. *Exp. Gerontol.* **45**, 738–743.

Varki A, Cummings R, Esko J, Freeze H, Stanley P, Bertozzi C, Hart G, Etzler M (2009). *Essentials of Glycobiology*, 2nd edn. New York: Cold Spring Harbor Laboratory Press.

Wang X, Inoue S, Gu J, Miyoshi E, Noda K, Li W, Mizuno-Horikawa Y, Nakano M, Asahi M, Takahashi M, Uozumi N, Ihara S, Lee SH, Ikeda Y, Yamaguchi Y, Aze Y, Tomiyama Y, Fujii J, Suzuki K, Kondo A, Shapiro SD, Lopez-Otin C, Kuwaki T, Okabe M, Honke K, Taniguchi N (2005) Dysregulation of TGF-beta1 receptor activation leads to abnormal lung development and emphysema-like phenotype in core fucose-deficient mice. *Proc. Natl Acad. Sci. USA* **102**, 15791–15796.

Wang X, Gu J, Ihara H, Miyoshi E, Honke K, Taniguchi N (2006a) Core fucosylation regulates epidermal growth factor receptor-mediated intracellular signaling. *J. Biol. Chem.* **281**, 2572–2577.

Wang X, Gu J, Miyoshi E, Honke K, Taniguchi N (2006b) Phenotype changes of Fut8 knockout mouse: core fucosylation is crucial for the function of growth factor receptor(s). *Methods Enzymol.* **417**, 11–22.

Wang X, Fukuda T, Li W, Gao CX, Kondo A, Matsumoto A, Miyoshi E, Taniguchi N, Gu J (2009) Requirement of Fut8 for the expression of vascular endothelial growth factor receptor-2: a new mechanism for the emphysema-like changes observed in Fut8-deficient mice. *J. Biochem.* **145**, 643–651.

Weindruch R, Naylor PH, Goldstein AL, Walford RL (1988) Influences of aging and dietary restriction on serum thymosin alpha 1 levels in mice. *J. Gerontol.* **43**, B40–B42.

Zhao Y, Itoh S, Wang X, Isaji T, Miyoshi E, Kariya Y, Miyazaki K, Kawasaki N, Taniguchi N, Gu J (2006) Deletion of core fucosylation on alpha3beta1 integrin down-regulates its functions. *J. Biol. Chem.* **281**, 38343–38350.

Supporting Information

Additional supporting information may be found in the online version of this article:

Fig. S1 *Fut8* expression, FUT8 protein levels and core-fucosylation in FUT8 KD sebocytes vs. control sebocytes.

Fig. S2 IGF-1-induced lipid synthesis after 48 h of stimulation.

As a service to our authors and readers, this journal provides supporting information supplied by the authors. Such materials are peer-reviewed and may be re-organized for online delivery, but are not copy-edited or typeset. Technical support issues arising from supporting information (other than missing files) should be addressed to the authors.